Special Issue – MICAP-2021

Muhsin A. Kudhier* and Roonak Abdul Salam A. ALKareem, Raad S. Sabry

Enhanced photocatalytic activity of TiO_2-CdS composite nanofibers under sunlight irradiation**

https://doi.org/10.1515/jmbm-2021-0022
Received Jul 20, 2021; accepted Sep 23, 2021

Abstract: Pure TiO_2 and TiO_2-CdS composite nanofibers were synthesized through electrospinning technique. The effects of various levels of CdS loading in a TiO_2 nanofibers composite were investigated. Pure TiO_2 nanofibers were polycrystalline with an anatase phase, whereas anatase and wurtzite phases coexisted in the TiO_2-CdS composite nanofibers, according to X-ray diffraction (XRD) measurements. Using field emission scanning electron microscopy (FESEM) and UV-Visible spectroscopy, the impacts of composite CdS nanoparticles with TiO_2 nanofibers were investigated. Pure TiO_2 nanofibers have a smooth surface with several microns in length and 21–48 nm in diameter, but when CdS nanoparticles are added, the surface becomes granular. The energy band gap (E_g) evaluated from UV-Visible spectroscopy reduced from a value of 3.70 eV for pure TiO_2 nanofibers to 1.70 eV for TiO_2-1CdS nanofibers. Photocatalytic properties of pure TiO_2 and TiO_2-CdS composite nanofibers were calculated by a methylene blue (MB) aqueous solution degradation under sunlight irradiation. The results revealed that TiO_2-0.5CdS nanofibers have efficient photocatalytic activity of up to 98 % after only 60 min.

Keywords: TiO_2-CdS composite, nanofibers, photocatalytic activity

1 Introduction

Among the several treatment options, photocatalysis is thought to be the most cost-effective, successful, and environmentally friendly way for completely degrading organic contaminants in waste water [1, 2, 3]. The importance of choosing proper photocatalysts that can absorb sunlight and separate photoexcited electrons from holes has been verified. TiO_2 is the most effective photocatalyst among the documented semiconductor photocatalysts, due to its remarkable photoactivity, nontoxicity, cheap cost, high stability, and water unsolvable qualities under most situations [4]. The adjustment of TiO_2 photocatalysts for increased light absorption and photocatalytic activity under sunlight irradiation has become a key research area in recent years due to the energy band gap value (3.2 eV) in the UV region.

On the other hand, component optimizations such as coupling semiconductors with narrower band gap materials, which can absorb visible light, are performed. With a narrow band gap of 2.4 eV, CdS has been used to composite with TiO_2 due to its visible-light response [5, 6]. CdS excitation wavelength is ≤ 516 nm, and it has clear positive aspects in terms of solar spectrum absorption. As a result, the TiO_2-CdS nanocomposites are not only stimulated by visible light, but the photoelectron-hole pairs' recombination possibilities are also limited [7, 8, 9].

One-dimensional nanostructures (1-D) of various oxide materials, such as nanowires, nanorods, nanotubes, and nanofibers, have gained a lot of interest in recent years. The massive quantity of thought is due to the critical scientific attention paid to these materials, in addition to their potential applications in a variety of practical instruments [10, 11, 12]. Electrospinning, in comparison to other technologies for generating nanofibers, has the benefits of the ability to control, simplicity, low-cost, and manageability in producing industrial amounts [13]. This method has an attractive potential for producing nanofibers from Polymers, Ceramics or Composites with diameters ranging from tens of nanometers to several microns. Furthermore, nanofibers diameter and length are controlled by the solution and processing parameters. The electrospinning technique has been widely employed to create oxide nanofibers [14, 15, 16].

***Corresponding Author: Muhsin A. Kudhier:** Physics Department, Education College, Mustansiriyah University, Baghdad, Iraq, E-mail: muhsinattia@uomustansiriyah.edu.iq
Roonak Abdul Salam A. ALKareem, Raad S. Sabry: Physics Department, Science College, Mustansiriyah University, Baghdad, Iraq

**Paper included in the Special Issue entitled: Proceedings of Mustansiriyah International Conference on Applied Physics – 2021 (MICAP-2021)

In the current study, TiO_2-CdS composite nanofibers samples were manufactured in a simple manner and evaluated using X-ray diffraction (XRD), field emission scanning electron microscopy (FESEM), and UV–Visible spectroscopy. Under sunlight irradiation, the photocatalyst exhibited high photoactivity for the destruction of MB. The results showed that MB was entirely degraded after 60 min of exposure to sunlight.

2 Materials and methods

2.1 Materials

Titanium tetraisopropoxide Ti $[OCH(CH_3)_2]_4$ (TIP), (96 %Sigma Aldrich), acetic acid (99.5%), ethanol (98%), polyvinylpyrrolidone (PVP)(Sigma Aldrich Molecular weight Mw = 1,300,000), ethylene glycol (EG), and thiourea were all purchased from (Scharlau, Spain), and cadmium chloride was purchased from ($CdCl_2$, 98 % Sigma Aldrich).

2.2 Synthesis of TiO_2 nanofibers

1 g of titanium tetraisopropoxide was mixed with 2 ml acetic acid and 2 ml ethanol to make a solution in a typical procedure. After resting for 10 minutes, the solution was mixed with 7 mL of PVP solution in ethanol. This PVP solution was held in a concentration of 10 wt%, and the combination that resulted was regularly stirred for 15 min. This final solution was directly injected into a syringe with a 21 gauge needle (used as the nozzle). The emitting electrode from a Gamma High Voltage Research ES30P power supply capable of generating direct current voltages of up to 25 kV was attached to the needle. The grounding electrode from the same power supply was attached to a plate of aluminum with clean glass substrates fixed on it, which was used as the collector plate and was placed 22 cm in front of the tip of the needle. From the nozzle, a fluid jet was ejected when a voltage of 20 kV was subjected across the needle tip and the collective plate. The fluid was fed at a rate of 1 ml/h, which was controlled by a syringe pump. The solvent evaporates as the jet advanced toward the collecting plate, leaving only extremely fine fibers on the collector plate, as seen in Figure 1. To permit whole hydrolysis of TIP, the produced fibers were exposed in a moisture bath for about 8 h and then calcined at 500°C for 3 hours at a rate of 10°C/min to eliminate any leftover PVP material.

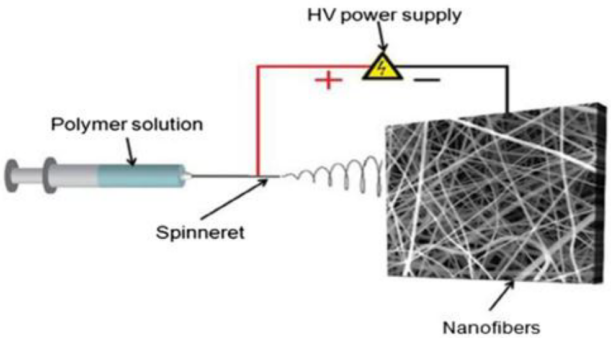

Figure 1: Diagram of electrospinning technique.

2.3 Synthesis of TiO_2-CdS composite nanofibers

Around (0.5, 1, 2) g of cadmium chloride $CdCl_2$ was dissolved into 12.5 ml ethylene glycol under continuous stirring at 70-80 ^oC. Around (0.67, 1.35, 2.7) g of thiourea was dissolved separately in 12.5 ml ethylene glycol and added to the above solution containing Cd ions drop wise. Now the obtained pure TiO_2 nanofibers samples were immersed in this final solution and the temperature was then increased to 100 ^oC and kept at this value for 2.5 h. The samples are then washed in water and ethanol. Finally, the three TiO_2-CdS samples with varying CdS concentrations were heated for 2 hours at 300 ^oC. TiO_2-*X*CdS composite nanofibers. The samples were generated with varying amounts of CdS, and the results were labelled as TiO_2-*X*CdS, where *X* is the molar concentration of CdS (*X* = 0.25, 0.5, and 1).

2.4 Characterization

2.4.1 XRD, UV-VIS, FESEM measurements

X-ray diffraction (XRD) technique was used to describe a crystalline phase of the produced TiO_2 and TiO_2-*X*CdS nanofibers, using X-ray diffractometer with CuKα1 (U.S. Monoger). A UV-Vis spectrophotometer (Shimadzu UV-1601) was used to record the absorption spectrum of pure TiO_2 and TiO_2-*X*CdS composite nanofibers. Also, field emission scanning electron microscope (FESEM; TESCAN MRI3) was used to observe the samples after being gold coated.

2.4.2 Photocatalysis studies

The degradation of an MB aqueous solution in a photochemical container was used to test the photocatalysis of pure TiO_2 and TiO_2-CdS composite nanofibers. The photo-

catalytic activity of TiO_2-CdS was measured using a 25 mg/L MB aqueous solution made with distilled water as a model pollutant. In a glass cup inclosing 50 mL of MB solution, 20 mg TiO_2-CdS composite nanofibers were introduced. To validate the establishment of desorption and adsorption equilibrium of MB on the TiO_2-CdS surface, the solution was placed in a photocatalytic container and stirred in the dark for 1 hour. Later, the suspension was exposed to sunlight. To maintain the suspension's stability, it was moderately stirred throughout the experiment. 4 mL of the suspension was removed at 10 min intervals and UV–Vis analysis was utilized to produce a time-dependent variation in the absorbance of the supernatant between 550 and 750 nm. The color change of MB was assessed by using a UV–Vis spectrophotometer standardized according to Beer Lambert's law to measure the absorbance value at λ = 664 nm.

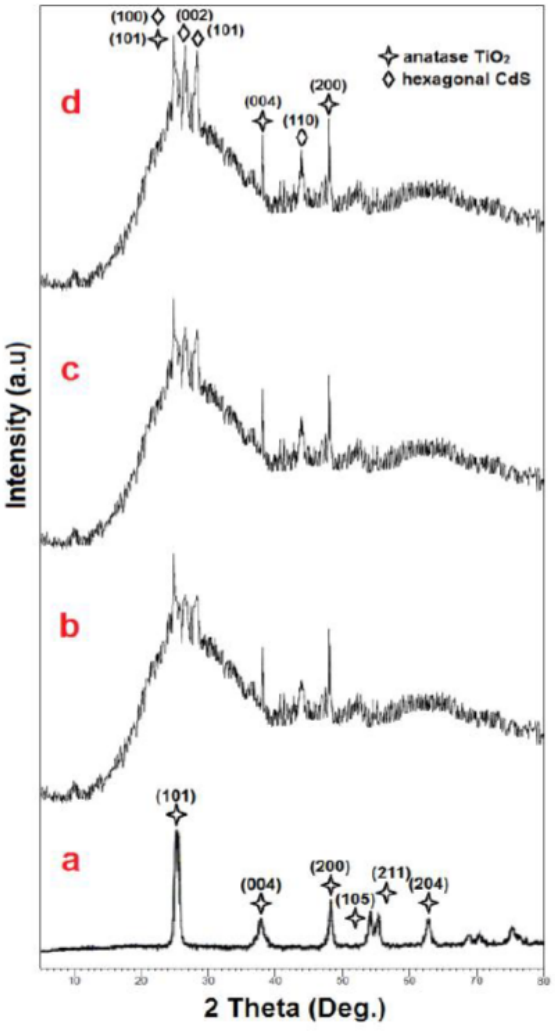

Figure 2: XRD spectra of (a) pure TiO_2 nanofibers, (b) TiO_2- 0.25CdS, (c) TiO_2- 0.5CdS, (d) TiO_2- 1CdS composite nanofibers.

3 Results and discussion

Figure 2 illustrates the XRD patterns of pure TiO_2 and TiO_2-*X*CdS nanofibers. The peaks in Figure 2a agree to the (101), (004), (200), (105), (211), and (204) planes of the TiO_2 anatase (tetragonal) phase. No peak for the rutile and brookite phases was distinguished, showing that the product samples are of high purity. Additional peaks appear in Figure 2b, c, and d, which belong to CdS hexagonal wurtzite phase, and correspond to the (100), (101), and (110) crystal planes. The intensity of hexagonal CdS peaks increased with the increasing of the molar concentration of CdS from 0.25 to 1. As a result, the XRD patterns obviously indicate the coexistence of pure TiO_2 anatase and CdS wurtzite phases.

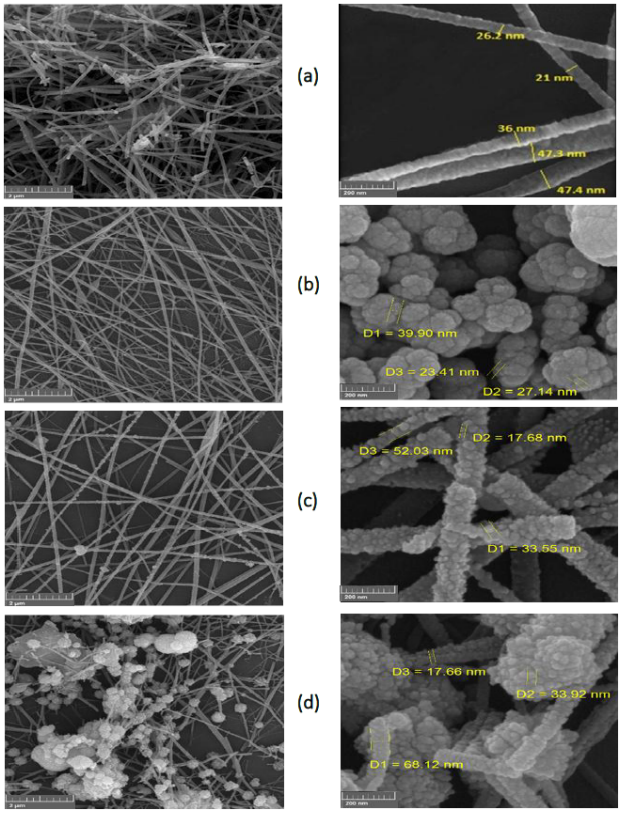

Figure 3: FESEM images of (a) pure TiO_2 nanofibers, (b) TiO_2-0.25CdS, (c) TiO_2-0.5CdS, and (d) TiO_2-1CdS composite nanofibers.

FESEM images of pure TiO_2 and TiO_2-*X*CdS nanofibers produced at various CdS molar concentrations are shown in Figure 3. Pure TiO_2 shows uniform fibers with a length of several microns and a diameter of 21–48 nm in Figure 3a. The as-synthesized products retain the nanofiber framework after composite with CdS, and there are abundant CdS nanoparticles (approximately 17–35 nm) attached outside

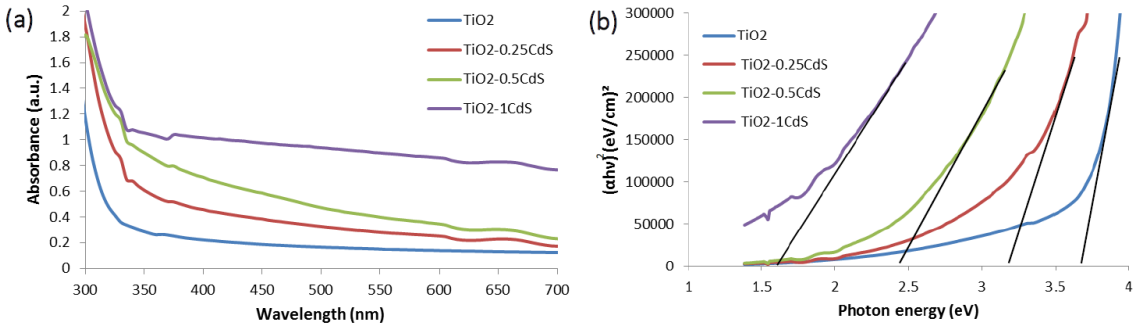

Figure 4: Absorbance versus wavelength of TiO_2 nanofibers prepared with various CdS loadings (b) allowed direct energy band gap of TiO_2 nanofibers prepared with various CdS loadings.

these TiO_2 nanofibers. The nanocomposites stoichiometry of CdS to TiO_2 and homogenous surface morphology are investigated using FESEM images. These micrographs reveal that the smooth surface of pure TiO_2 nanofibers changes to granular surface when adding CdS nanoparticles. This situation indicates that CdS nanoparticles stick on the surface of the fibers as clearly shown in Figures 3b, c, and d, and definitely increased the total surface area and this result is critical for the use of photocatalytic activity.

The UV–Vis absorbance spectra of pure TiO_2 and CdS–TiO_2 composites are shown in Figure 4a. As demonstrated in this Figure, adding CdS to TiO_2 increases its absorbance under sunlight, and the absorption intensity of the CdS–TiO_2 samples improves as the amount of CdS increases, owing to CdS's higher photocatalytic activity and narrower energy band gap than TiO_2. Semiconductor materials absorb light less than a threshold wavelength (fundamental absorption edge λ_g) [17], and it is clear that pure TiO_2 has the absorbing edge below 330 nm, whereas the shift to visible region reaches 350 nm for TiO_2-0.25CdS and TiO_2-1CdS, and continues to increase to 375 nm for TiO_2-0.5CdS and TiO_2-1CdS. As shown in Figure 4b, the band gap reduces from 3.70 eV for TiO_2 nanofibers to 3.05 eV for TiO_2-0.25CdS nanofibers and then to 1.70 eV for TiO_2-1CdS nanofibers. All results indicate that adding CdS nanoparticles to TiO_2 considerably improve its visible light absorption capabilities [18]. Photocatalytic degradation results display a considerable improvement in the photocatalytic effectiveness of TiO_2-CdS nanocomposites, owing to the combined effect of enhanced charge carrier life time and the major function of sulphate species found at the surface [7].

Figures 5 and 6 show the yield of MB during photocatalytic testing as a function of irradiation time. The results obviously specify that the photocatalytic performance of TiO_2 can be seriously enhanced by introducing inorganic CdS semiconductor into TiO_2 structure. When CdS nanoparticles contact with TiO_2 nanofibers, the electrons at the TiO_2-CdS interface would rearrange and migrate from CdS to TiO_2, leaving holes on the CdS. Then a depletion layer can be formed on CdS surface, while an accumulation layer can be formed on TiO_2 surface, leading to the formation of the internal electric field at the interface. The internal electric field, directing from the CdS surface to the TiO_2 surface, restrained the further migration of electrons. Finally, the two Fermi levels reach the same level and the mobility of electron from CdS to TiO_2 reaches equilibrium [19]. Figure 6 shows the time-dependent photodegradation of MB in pure TiO_2 and TiO_2-*X*CdS nanofibers when exposed to sunlight.

The following relationship was used to compute the photodegradation efficiency for each test, as shown in Figure 7:

$$\text{Efficiency (\%)} = \frac{Co - C}{Co} \times 100\%$$

where efficiency (%) is the photodegradation efficiency, C_0 is the concentration of MB before illumination, and C is the concentration of MB in the suspension after time t (mg/L).

The pseudo first-order rate constant k (min^{-1}) can be calculated using the slope of the line from Figure 8.The value of k is 0.0120 min^{-1} for pure TiO_2 and 0.0362, 0.0525, 0.0159 min^{-1} for TiO_2-0.25CdS, TiO_2-0.50CdS, TiO_2-1CdS nanofibers respectively.

TiO_2 nanofibers' efficiency (after 60 minutes) is 50%, while of TiO_2-0.25CdS is 94% and 98% for TiO_2-0.5CdS nanofibers, but this value is higher than that of TiO_2-1CdS which is 63%. The highest efficiency value was obtained by using (TiO_2-0.5CdS) nanofibers and the reason can be attributed to the value of the energy gap in this case (2.45 eV) which corresponds to the absorption edge (506 nm) and this value is approximately in the middle of the visible region and most appropriate and preferred for absorbing visible light, while the other values of the energy gap which are due to (TiO_2-0.25CdS) and (TiO_2-1CdS) nanofibers are on the edge of the visible region (400 nm and 775 nm) re-

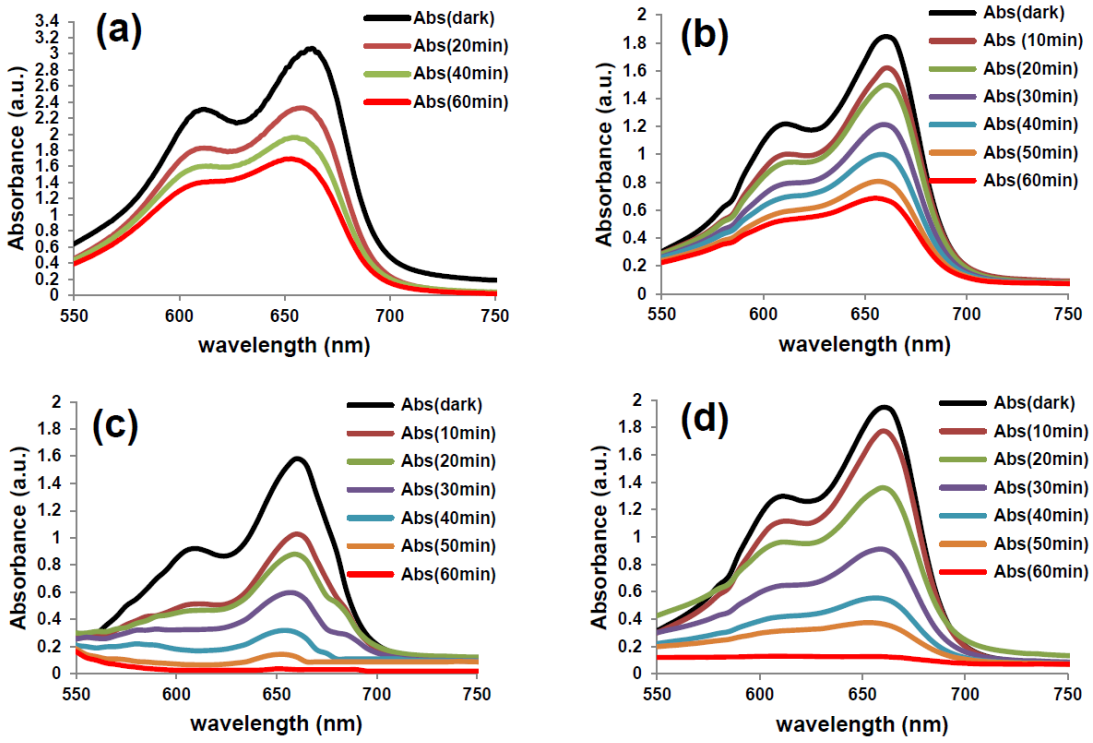

Figure 5: UV-Vis photocatalytic absorption spectrum of MB recorded by TiO_2 photocatalyst prepared with various intervals. (a) pure TiO_2 nanofibers (b) TiO_2-0.25CdS (c) TiO_2-0.5CdS (c) TiO_2-1CdS composite nanofibers.

Table 1: Fundamental results for pure TiO_2 and TiO_2-CdS nanofibers.

Sample	absorption edge λ_g (nm)	Energy gap E_g (eV)	k (min^{-1}) $\times 10^{-4}$	Efficiency (%) (after 60 min)
Pure TiO_2	340	3.65	120	50
TiO_2-0.25CdS	400	3.10	362	94
TiO_2-0.5CdS	506	2.45	525	98
TiO_2-1CdS	775	1.60	159	63

spectively. The efficiency obtained in this research is very high when compared to other researches. Gomathi Thanga Keerthana *et al.* [20] obtained an efficiency amounted to 77% after 180 min, while the efficiency amounted to 85.9% after 120 min in the research carried out by Makama *et al.* [21]. Table 1 summarizes the fundamental results for pure TiO_2 and TiO_2-CdS nanofibers.

4 Conclusions

Electrospinning was used to successfully produce TiO_2-CdS nanocomposites with various CdS loadings in order to examine the photocatalytic activity of these materials as a function of CdS relative quantity. UV-Vis tests show that CdS–TiO_2 composite nanofibers extend the absorption band edge in the visible range. The addition of CdS nanoparticles to TiO_2 nanofibers dramatically improves the photocatalytic activity. TiO_2-0.5CdS composite nanofibers displays the best photocatalytic activity under sunlight and the efficiency reaches 98% after only 60 min. The as-synthesized TiO_2-CdS composite nanofibers exhibit better photoactivity under sunlight irradiation than that of pure TiO_2.

Acknowledgement: The authors are appreciative for the support they received from Physics Department, Sciences College, Mustansiriyah University for supported this work. should be: Acknowledgement: The authors appreciate the support from Physics Department, Sciences College, Mustansiriyah University.

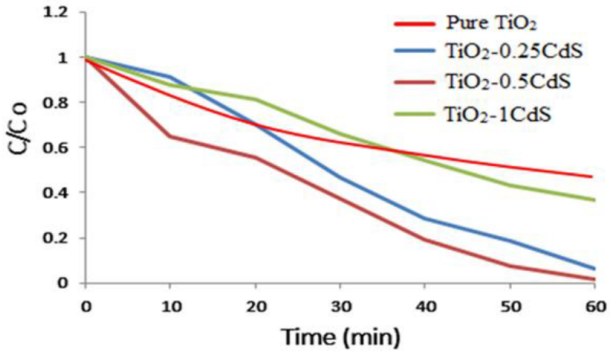

Figure 6: Time-dependent photodegradation of MB in the presence of pure TiO_2 and a composite with varying CdS loadings under sunlight irradiation.

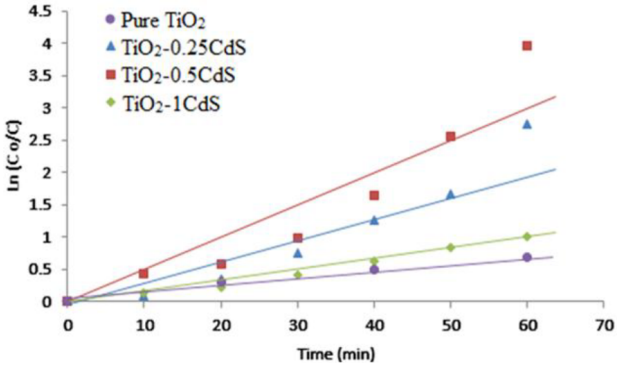

Figure 8: The degradation of (MB) in the first order kinetics as a function of irradiation duration of pure and composite TiO_2 with various CdS loadings.

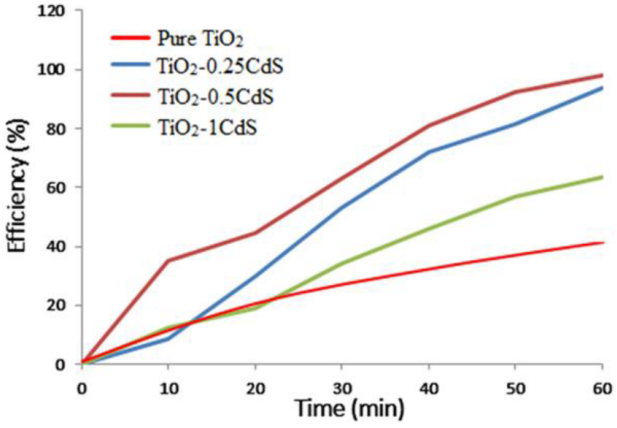

Figure 7: Efficiency of MB degradation using pure and composite TiO_2 with various CdS loadings.

Funding information: The authors state no funding involved.

Author contributions: All authors have accepted responsibility for the entire content of this manuscript and approved its submission.

Conflict of interest: The authors state no conflict of interest.

References

[1] Sobhani AN, Behpour M. Synthesis, characterization, and morphological control of $Eu_2Ti_2O_7$ nanoparticles through green method and its photocatalyst application. J Mater. 2016;27:11946.

[2] Kudhier MA, Sabry RS, Al-Haidarie YK. Novel and simple method to synthesize donut-like TiO_2 with photocatalytic activity. Mater Sci Semicond Proc. 2018;73:35.

[3] Dang R, Xiangrong M. CdS nanoparticles decorated anatase TiO_2 nanofibers with enhanced visible light photocatalytic activity for dye degradation, J Mater Sci Mater Electron. 2017;28:8818.

[4] Sabry RS, Al-Haidarie YK, Kudhier MA. Synthesis and photocatalytic activity of TiO_2 nanoparticles prepared by sol–gel method. J Sol-Gel Sci Technol. 2016);78:299.

[5] Zhang J, Wageh S, Al-Ghamdi A, Yu J. New understanding on the different photocatalytic activity of wurtzite and zinc-blende CdS. Appl Catal B Environ. 2016;192:101.

[6] Hussein EH, Mohammed NJ, Al-Fouadi AH, Abbas KN, Alikhan JS, Maksimova K, Goikhman AY. Impact of deposition temperature on the structural properties of CdS/Si nanoparticles for nanoelectronics. Mater Lett. 2019;254:282.

[7] Hamdi A, Ferreira DP, Ferraria MA, Conceição DS, Vieira LF, Carapeto AP, Boufi S, Bouattour S , Botelho do Rego MA. TiO_2-CdS Nanocomposites: Effect of CdS Oxidation on the Photocatalytic Activity. J Nanomater. 2016;1:1

[8] Wang X, Liu G, Wang L, Pan J, Lu GQ, Cheng HM. TiO2 films with oriented anatase 001 facets and their photoelectrochemical behavior as CdS nanoparticle sensitized photoanodes. J Mater Chem. 2011;21:869.

[9] Zou Z, Qiu Y, Xie C, Xu J, Luo Y, Wang C, Yan H. CdS/TiO_2 nanocomposite film and its enhanced photoelectric responses to dry air and formaldehyde induced by visible light at room temperature. J Alloys Compd .2015;645:17.

[10] Kathavate VS, Amudha K, Adithya L, Pandurangan A, Ramesh NR, Gopakumar K. Mechanical behavior of composite materials for marine applications – an experimental and computational approach. J Mech Behav Mater. 2018;27:1.

[11] Yu G, Cao A, Lieber CM. Large-area blown bubble films of aligned nanowires and carbon nanotubes. Nat Nanotechnol. 2007;2:372.

[12] Aifantis KE, Hackney SA. An Ideal Elasticity Problem for Li-Batteries, J Mech Behav Mater. 2003;14(6):413.

[13] Lu W, Lieber CM. Nanoelectronics from the bottom up. Nat Mater. 2007;6:841.

[14] Su Y, Lu B, Xie Y, Ma Z, Liu L, Zhao H, Zhang J, Duan H, Zhang H, Li J, Xiong Y, Xie E. Nanocomposites for Musculoskeletal Tissue Regeneration. Nanotechnology. 2011;22:285609.

[15] Liu Z, Sun DD, Guo P, Leckie JO. An Efficient Bicomponent TiO_2/SnO_2 Nanofiber Photocatalyst Fabricated by Electrospinning with a Side-by-Side Dual Spinneret Method. Nano Lett.

2007;7:1081.

[16] Munir MM, Iskandar F, Yun KM, Okuyama K, Abdullah M. Optical and electrical properties of indium tin oxide nanofibers prepared by electrospinning. Nanotechnology.2008;19:145603.

[17] Usubharatana P, McMartin D, Veawab A, Tontiwachwuthikul P. Photocatalytic Process for CO_2 Emission Reduction from Industrial Flue Gas Streams. Ind Eng Chem Res. 2006;45:2558.

[18] Beigi AA, Fatemi S, Salehi Z. Synthesis of nanocomposite CdS/TiO_2 and investigation of its photocatalytic activity for CO_2 reduction to CO and CH_4 under visible light irradiation. J CO_2 Util. 2014;7:23.

[19] Meng A, Zhu B, Zhong B, Zhang L, Cheng B. Direct Z-scheme TiO_2/CdS hierarchical photocatalyst for enhanced photocatalytic H_2-production activity. Appl Surf Sci. 2017;422:518.

[20] Keerthana BT, Murugakoothan P. Synthesis and characterization of CdS/TiO_2 nanocomposite: Methylene blue adsorption and enhanced photocatalytic activities. Vacuum .2019;159:476.

[21] Makama AB, Salmiaton A, Saion EB, Choong TSY, Abdullah N. Synthesis of CdS Sensitized TiO_2 Photocatalysts: Methylene Blue Adsorption and Enhanced Photocatalytic Activities. Int J Photoenergy. 2016;2016:1.